Reactor Parametric Assessments for Alternative Propellant Nuclear Thermal Propulsion Engines

Corey Smith[1], Daria Nikitaeva[1], Jacob Stonehill[1], Matthew Duchek[2]

[1]*Advanced Projects Huntsville, Analytical Mechanics Associates, Huntsville, AL, 35806*
[2]*Advanced Projects Denver, Analytical Mechanics Associates, Denver, CO, 80211*

Primary Author Contact Information: 678-739-8494, corey.d.smith@ama-inc.com

[Placeholder for Digital Object Identifier (DOI) to be added by ANS]

This work focuses on the implications of alternative working fluids for nuclear thermal propulsion (NTP) reactors. To perform this analysis, NASA's Testing Reference Design (TRD) is altered using parametric studies with selected alternative propellants to determine the reactor modifications required to enable an operable system. This research investigates ammonia, water, methane, helium, and enriched diborane as feasible options to enable a specific impulse (I_{sp}) greater than the chemical propulsion alternatives. Frozen and dissociated I_{sp} for each propellant is shown for variable chamber temperature conditions. Geometrical sensitivities are performed to observe the impact on the neutron multiplication factor (k_{eff}), system mass, and HALEU loading. Control drum worth curves are included for 5-degree increments of rotation. The base TRD configuration does not enable a critical system for ammonia and enriched diborane, thus these propellants will be highlighted in the final results. Equivalent study results for hydrogen will be included as a point of comparison to the performance of the other options.

I. INTRODUCTION AND MOTIVATIONS

Government and commercial entities have a vested interest in novel propulsion techniques to enable cislunar and interplanetary human space travel. One of the primary options under investigation by NASA's Space Nuclear Propulsion (SNP) project is nuclear thermal propulsion (NTP) which relies on an extreme temperature reactor heat exchanger coupled with a modern expander engine cycle. To improve the performance of the propulsion system, the primary propellant option for NTP is hydrogen (H_2), with the engine using it referred to in this work as H-NTP, which optimizes the specific impulse (I_{sp}) of the engine. The current government baseline reactor and engine configuration, referred to as the Testing Reference Design (TRD), relies on H-NTP to enable approximately a thrust of 15 klbf and a I_{sp} of 900 seconds[9]. This design, as discussed in Section II, utilizes an expander engine cycle to heat hydrogen from a cryogenic storage tank to 2700 K. The reactor choice for the TRD is a lattice of ceramic-ceramic (CERCER) fuel assemblies with internal flow channels interspersed within a zirconium hydride moderator block configuration.

While H-NTP dominates for crewed Martian missions, other propellant options can be scrutinized for different architectures, such as cislunar tugs and Martian cargo missions. In addition, numerous technical and programmatic challenges for hydrogen are present and decrease its viability for more routine missions. These concerns include including cryogenic storage, hot hydrogen attack through chemical incompatibility, and ground testing limitations due to combustibility. Overcoming these inherent challenges will require novel reactor design techniques or a sacrifice of performance with the use of an alternative propellant. This work will investigate some of these secondary working fluid options that are feasible for alternative propellant nuclear thermal propulsion (A-NTP) engines while maintaining elevated system performance.

I.A. Alternative Propellant Options

Alternative propellants were selected for this study based upon the following attributes: critical state, carbon/oxygen concentration, molecular weight, boiling point, storage temperature range, and liquid density. These parameters are of interest because they inform overall engine performance, chemical compatibility and corrosion, and tank operating conditions. Here, the maximum liquid storage range (regardless of storage pressure) is between the freezing temperature and the critical point temperature. High critical temperatures will require additional preheating within the engine cycle to support turbine operation. High critical pressures will require high cycle pressures which will increase the engine mass. High liquid densities will result in lower tank masses; however, they are usually associated with high molecular weight propellants which will require higher propellant mass from the resulting lower specific impulse.

As Table I shows, the selected propellants for investigation include H_2, ammonia (NH_3), water (H_2O), methane (CH_4), helium (He), and diborane (B_2H_6). While H-NTP has the overarching challenges mentioned previously, helium is much more difficult to store than hydrogen due to its extremely low liquid temperature[2], dissociated methane will leave carbon residue[3] (i.e. coking), and ammonia and water require significant pre-heating prior to the engine turbomachinery. Water can also lead to corrosion via rusting within engine turbomachinery,

in-core flow channels, and in the nozzle region[6]. In addition, diborane will negatively impact the in-core neutronics without substantial enrichment, thus all uses in this model consist of a 99.9% B-11 enriched diborane propellant. Additional enrichment may be required if reactor performance is impacted substantially by the parasitic B-10 isotope.

TABLE I. Selected Alternative Propellants

Chemical Formula	Molecular Weight (g/mol)	Freezing Temperature (K)	Critical Point (K, MPa)	Liquid Density (kg/m^3)
H_2	2.018	14	33, 1.3	70.8
NH_3	17.031	195	405, 11.4	730
H_2O	18.015	273	647, 22	997
CH_4	16.043	91	190, 4.6	657
He	4.003	-	5.2, 9.3	124.8
B_2H_6	27.670	108	289, 4	1220

I.B. Specific Impulse Comparison

Alternative NTP propellants will have a considerable impact on the achievable specific impulse of the engine. Assuming an ideal, isentropic expansion process, Eq. 1 shows the relationship for I_{sp} as a function of the propellant's molecular weight (mw) and specific heat ratio (γ) as well as the chamber temperature (T_c). In addition to varying the molecular weight between each considered propellant, the high operating temperatures of an NTP system can cause some propellants to fully dissociate, decreasing average mw and increasing the I_{sp}.

$$I_{sp} = \frac{v_e}{g_0} = \frac{1}{g_0}\sqrt{\frac{2\gamma}{\gamma-1}\frac{\Re T_c}{mw}\left[1-\left(\frac{P_e}{P_C}\right)^{\frac{\gamma-1}{\gamma}}\right]} \quad (1)$$

Fig. 1 shows the specific impulse at various chamber temperatures for each propellant. Here, both methane and diborane are assumed to be fully dissociated due to their fast chemical kinetics and the high temperatures associated with the NTP reactor. The typical combustion chamber temperature of chemical engines is around 3500 K which is significantly higher than what the NTP engine can produce due to fuel material temperature limitations. Hydrogen and oxygen chemical engines can produce thrust at a I_{sp} of around 450 seconds[1]. At the TRD temperature of 2700 K, helium, diborane, and fully dissociated methane outperform chemical engine systems. Methane and oxygen chemical engines can produce thrust at a I_{sp} of 365 seconds[1] which is where both water and ammonia operate at the TRD chamber temperature of 2700 K (Ref. 4). Ammonia will likely slightly dissociate at this temperature; therefore, ammonia's I_{sp} is expected to be slightly higher than presented in Fig. 1 due to its decreased average MW.

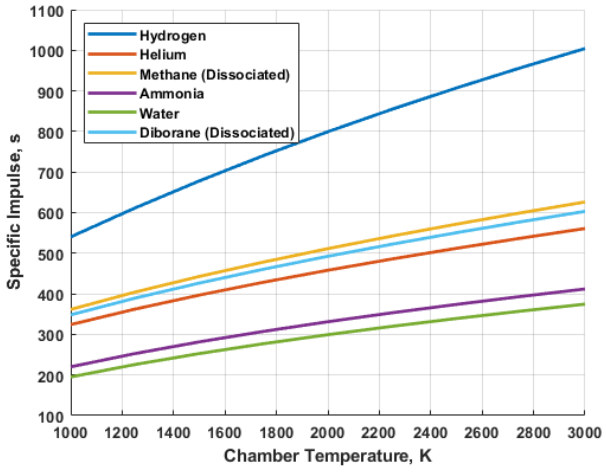

Fig. 1. Specific Impulse for Various A-NTP Propellants

II. METHODOLOGY

II.A. A-NTP Engine Cycles

The engine cycle should cater to the fluid with which it works and a large factor which determines the details of the fluid flow is the liquid temperature range (the difference between the freezing and critical temperatures). The baseline NTP TRD expander cycle shown in Fig. 2. Details of this cycle are presented in a different paper[5]. This cycle is catered to hydrogen which has a very narrow liquid temperature range. Because of this, a boost pump (between States 1 and 2) is required prior to the main pumps (between States 2 and 3) to discourage cavitation at the Main Pump inlet. Furthermore, the enthalpy gained from flowing through the Regenerative cooling (States 6 to 7), control drum/reflector cooling (States 7 to 8), and moderator block cooling (States 10 to 11) will be enough to provide a supercritical fluid to the turbine circuits (States 13 through 19) and ensure margin to avoid the fluid from transitioning back to a liquid at the turbine exit. This same cycle will work for helium and potentially methane due to the narrow liquid ranges of these propellants.

Propellants with broader liquid temperature ranges will require preheating to achieve a supercritical state prior to entering the turbines. While simplistic to model from a thermal hydraulic perspective, current NTP designs are not readily capable to enable preheating from a thermo-structural and possible neutronics perspective. A beneficial biproduct of preheating is the reduction for the need of a Boost Pump, as shown in Fig. 2. A key change in this cycle is that the flow no longer splits between cooling the control drums/reflector and moderator block; instead, the fluid flows serially. Furthermore, the flow then goes through a portion of the fuel elements to become preheated for the turbines. This results in high pressure losses which will require additional pump stages and increase the mass of the non-nuclear engine components. This cycle is valid for all propellants in Table I except for hydrogen, helium, and potentially methane.

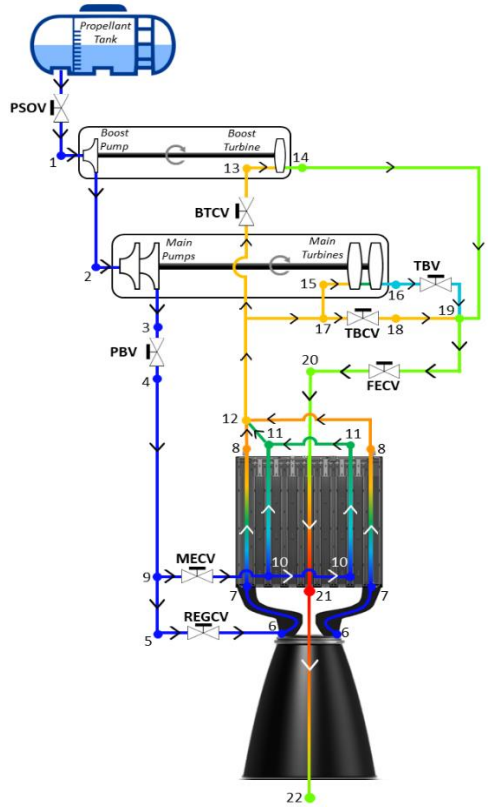

Fig. 2. NTP Testing Reference Design Engine Schematic

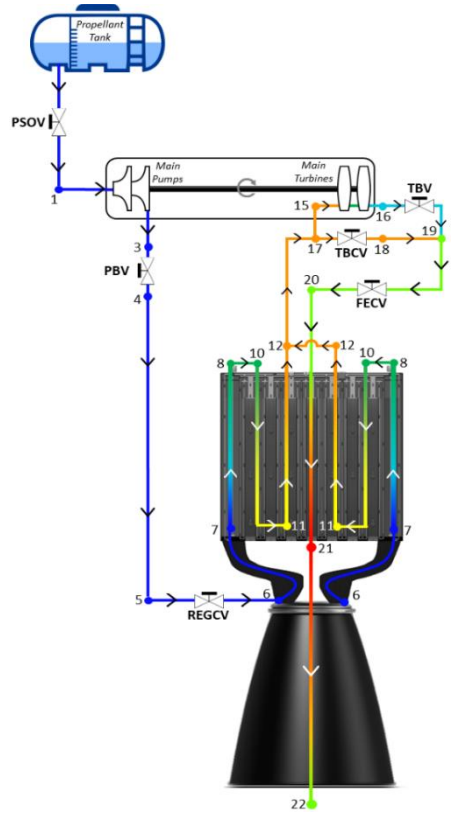

Fig. 3. A-NTP Preheating Engine Design Schematic

II.B. A-NTP Reactor Algorithm

To assess the alternative propellants in this study, the developed reactor modeling methodology can run extensive parametric sensitivities for a large number of test cases through coupled thermal hydraulic and neutronic analysis. Reactor analyses can be performed independently or through coupled calculations in the engine cycle to predict system-level performance. The base reactor unit cell geometry is taken from the TRD, but other parameters are allowed to vary to reach a critical mass. This option uses a moderator block configuration with circular fuel assemblies (FAs) interspersed in a circular lattice with internal coolant channels for convective heat removal. Since this hydrogen working fluid design does not rely on preheating, some variations are required to enable this new function for diborane, ammonia, and water.

The preheating thermal hydraulic in the reactor algorithm is based on a ring-by-ring methodology to increase the fluid enthalpy and reach a supercritical state prior to the turbine. In this work, the first and second rings around the central fuel assembly are designated as the preheat rings while the remaining assemblies serve as the superheat component of the reactor heat exchanger. Advantages for this approach include the inherent modularity of the active core. Designers can easily vary the amount of fuel assemblies that would be required to pre-heat without varying the coupled engine/reactor methodology. An expected benefit is with neutronic performance since there is lower temperature and density gas in the fuel assemblies. This will allow for additional reactivity control and power profile shaping capabilities without significant redesign.

Drawbacks include a required two-stage aft plenum and large pressure losses associated with 180° turns. For the plenum, reactor designs will need a large open plenum to incorporate the moderator channel exhaust across the geometry with specific open fuel assemblies for forced flow. This plenum would also include super-heat FA exhaust nozzles to the nozzle chamber. Both of these problems would require experimental understanding of the pressure losses for the 180° turn in the plenum and introduced turbulence from the crossflow exhaust nozzles.

The control and parametric variables in this work are:

Control Variables

- Reactor Unit Cell: Uses TRD values for radius, number of coolant channels, fuel type, and clad/structural/insulator layer thicknesses[9].
- Reflector Thickness: While this is a value that can be varied for point designs, it is held constant in this work to provide some consistency to the baseline design.

- Control Drum Quantity and Geometry: Number of control drums and the geometry of the poison vane/drum meat is constant as described in the TRD.
- Subcomponent Geometry: Each reactor configuration will include constant geometry for the axial reflectors, internal shielding, thermal plates, reactor pressure vessel, and fore plenum/vessel domes.

Parametric Variables

- Working Fluid: The primary investigation is the working fluid choice based on the desired propellant. Preliminary studies in this work will be focused on the reactor physics behavior (criticality assessment).
- Fuel Volume Loading: The use of a CERCER fuel form allows the designer to vary the fuel to matrix volume fraction in the fuel assembly. Radial variations of this value on a ring-by-ring basis are crucial to flatten the power peaking and increase the engine I_{sp}.
- Active Core Radius: Varying the fuel assembly pitch and active core radius will allow for varied neutronic performance as a function of the fuel to moderator ratio. These changes will also change the neutron leakage and system mass.
- Active Core Length: By maintaining a constant reactor unit cell, another knob that can be turned is the reactor length. Increased length will allow for improved neutronic performance from increased fuel volume and reduced neutron leakage while also increasing the residency time of the working fluid in all in-core flow channels. Mass penalties will be introduced by the increase in core volume.
- Control Drum Rotation: Simple parametric analyses can be performed on the control drum worth for each propellant choice by rotating the control drums. This will vary the amount of excess reactivity and shutdown margin the core will possess which will determine the reactor's controllability.

Variations on these parameters have a direct impact on the moderator to fuel ratio (MFR) of the reactor system which will be shown throughout Section III.B of this work. Most terrestrial and heritage space reactors operate under-moderated to avoid positive reactivity feedback during power increases or other transient events. However, results from this algorithm will show that the reactor performance can be worse when using a large MFR reactor design. Finding an optimal reactor geometrical configuration will minimize system mass and provide inherent safety for unexpected transients, such as water immersion.

II.C. Neutronics Input Generators

To create on-the-fly Serpent[10] input files based on the desired parametric sweep, a comprehensive input file generator has been developed in MATLAB. Rather than having to update each input file for every case, the input generator takes key input values from the user and automatically generates all relevant files with associated physics, geometry, and material cards. This model has been generated in MATLAB to increase its applicability to the Simulink-based X-NTP engine model[5,6,8]. To run the Monte Carlo simulation properly, the input generator must apply all relevant materials and physics to the simulated geometry. The geometry is generated by user defined dimensions of the active core, fuel assemblies, and all subcomponents.

The material card generator possesses a complex architecture of information building blocks that combine to form any material based on their constituent atoms and volume fractions. A data structure for each element has been created to hold its natural isotope abundances and atomic mass. The user can override the natural isotope abundances to yield an enriched material, as expected with the fuel material and diborane working fluid. If a porosity value (P) exists in the optional parameters, then the code applies a density correction to the theoretical density (ρ_{TD}), as shown in Eq. 2 known as the porosity correction step. The material card generator calculates the mass density of the mixture (ρ_{mix}) using a simple mixture formula based on Eq. 3 which occurs after the porosity correction step. The code then calculates the fraction of each i^{th} isotope in the mixture ($f_{m,i-mix}$) using the molecular formula, isotope mass (m_i), fractional abundance of the i^{th} isotope ($f_{i,a/o}$), and the mixture fraction of the i^{th} molecule ($f_{m,i-molecule}$).

$$\rho = \rho_{TD}(1 - P) \tag{2}$$

$$\rho_{mix} = \frac{1}{\sum_{i=1}^{n} \frac{f_{mass,i}}{\rho_i}} \tag{3}$$

$$f_{m,i-mix} = f_{m,i-molecule} N_{Avogadro} \frac{f_{i,a/o} m_i}{MW} \tag{4}$$

An optional parameter for material temperature directs the input generator to not only print out this temperature value with the material card, but to also adjust the suffix attached to the end of the isotope atomic number (Z) and atomic mass (A) identification (ID) number (ZAID). This suffix points Serpent to the appropriate neutron cross section database to improve underlying assumption in the model. Table II shows the library options and their temperature range of applicability.

TABLE II. Lib80x Library Temperature Ranges[7]

Library Suffix	Minimum Temperature (K)	Maximum Temperature (K)
.00c	293.6	600
.01c	600	900
.02c	900	1200
.03c	1200	2500
.04c	2500	-
.05c	0.01	250
.06c	250	293.6

III. RESULTS AND DISCUSSION

By implementing the engine and reactor algorithms discussed in Section II, several key sensitivities can be performed to observe the neutronic impacts as a result of drum swing and geometry changes. Prior to investigating these parametric changes, the first presented result is the neutron multiplication factor of each alternative propellant based on the baseline TRD configuration. In addition, the preheating assumption for each working fluid is included as well. These results are shown in Table III below. These preliminary results show that enriched diborane and ammonia are not able to reach a critical mass given the baseline configuration. While ammonia does have a substantial quantity of moderating hydrogen in the molecule, nitrogen possesses an absorption cross-section for thermal neutrons, leading to the decrease in criticality. Natural diborane was removed from the trade space due to the significant parasitic absorption of thermal neutrons in B-10, yielding a k_{eff} of approximately 0.25 for the baseline reactor. In addition, the neutron multiplication factors for helium, methane, and water all exceed the hydrogen benchmark value. Thus, the reactor geometry may be optimized for these propellant options to decrease the overall system mass, but these results will not be included in this work. The results for enriched diborane and ammonia will be the primary focus in subsequent sections of this report.

Both water and ammonia are examined with this cycle in detail in prior work[6]. Key findings included that the oxygen content in water will yield to rapid engine deterioration at temperatures close to those found in the TRD resulting in a low engine life. Both propellants increase the engine thrust should the reactor power stay the same at the expense of a low I_{sp}. As seen in Table III, these thrust values are roughly twice as much as those of the TRD H-NTP designs; however, the vehicles will be much heavier due to propellant mass and burn durations will be longer despite the increase in thrust due to the lower I_{sp}, as prior work has shown[7].

TABLE III. A-NTP Neutron Multiplication Factors and Engine Performance for the Baseline TRD Geometry

Propellant	Preheat Required?	k_{eff}	I_{sp} (s)	Thrust (klbf)
H_2	No	1.00130 ± 0.00039	900.0	15.0
NH_3	Yes	0.98503 ± 0.00037	369.5	24.8
He	No	1.00876 ± 0.00038	511.4	27.4
H_2O	Yes	1.01515 ± 0.00040	335.9	28.0
CH_4	Yes	1.00709 ± 0.00036	571.1	19.7
B_2H_6	Yes	0.95616 ± 0.00038	546.2	21.0

III.A. Control Drum Worth and Shutdown Margin

Following the preliminary results presented in Table III, the first simple parametric sensitivity focuses on the control drum worth and shutdown margin of the engine. Rotating the poison vane of the drums from completely outward facing (rotation angle of 0°) to inward facing (rotation angle of 180°) will showcase how much reactivity insertion the drums possess within the reactor. This sensitivity perturbed the drum rotation angle in increments of 5° between fully out and fully in to display the trends for each propellant. Results of this sensitivity can be seen in Fig. 4. The hydrogen curve, shown in black, serves as the datum for the other alternative propellants. The magnitude of the control drum worth is relatively constant for each option. Concerns over shutdown margin for helium, water, and methane may be present for off-nominal reactor transients, such as one or more stuck drum failures. Core designers may wish to update the core configuration similar to ammonia and enriched diborane to provide more safety margin. Ammonia and enriched diborane are shown to be subcritical for the baseline TRD and all drum rotation angles. To enable a critical system, core designers may vary the core length and radius, reflector thickness, fissile material volume, and/or fuel assembly pitch. These changes will impact the MFR, so additional investigation into this phenomenon is shown in Section III.B.

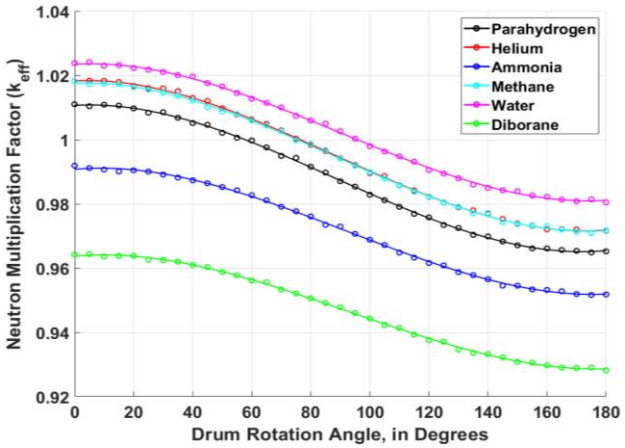

Fig. 4. Control Drum Worth Curves for Each Propellant

III.B. Geometry Parametric Analyses

Given that the reactivity insertion due to control drum rotation of each of the propellant options is well understood from Fig. 4, an additional sensitivity for ammonia and enriched diborane is performed by varying the radius and length of the active core for the TRD drum rotation angle and fuel volume loading pattern. This analysis investigates how the neutron multiplication factor and MFR will vary for active core radii between 28 and 36 cm and active core lengths between 100 and 140 cm. All subcomponents (e.g., pressure vessel, shields, plena, etc.) around the core are scaled accordingly. Fig. 5 shows the results for ammonia.

Some key observations from this analysis include that it is feasible to reach a critical system by simply varying the reactor size. Core designers will need to balance the system mass, shutdown margin, and other safety metrics prior to deciding on which radius/length pairing is ideal for this propellant. A relative extrema in the contour trend curves can be observed around a radius of 29 cm at all simulated lengths. This extrema represents where the core transitions from under- to over-moderated since increases to the active core radius will lead to more moderation given the same volume of fissile material. Thus, increasing the core radius above 29 cm will lead to a decrease in core reactivity due to the neutron lifetime. Increases to core length will see increases in criticality due to the increased fissile volume. Taller reactors will also see a decrease in the MFR. The final observation is that the system mass will vary as well with these curves given that the geometry is changing. Logically, the lowest reactor mass is observed in the bottom-left corner and the largest is in the top-right corner since the mass will scale with both the active core length and radius.

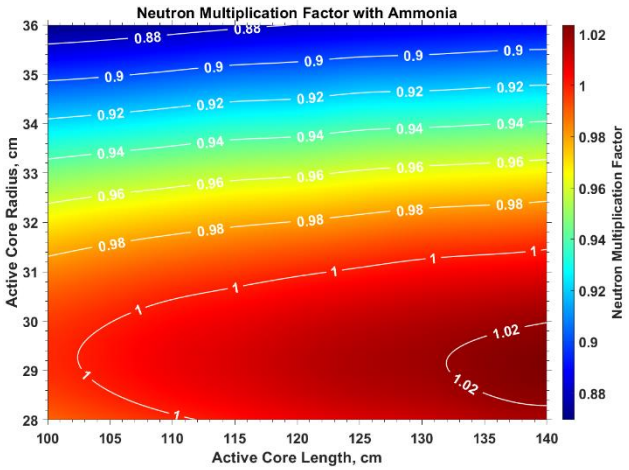

Fig. 5. Geometry Impacts on k_{eff} for Ammonia

Following the results of Fig. 5, an equivalent analysis is performed using an enriched diborane working fluid. As seen in Table III, the k_{eff} of this option is substantially below the other options. Results for this assessment are shown in Fig. 6. Initial takeaways from Fig. 6 show that the neutron multiplication factor will not reach unity without additional design changes beyond the geometry. Additional observations include that the MFR peak seen previously in Fig. 5 is also present for enriched diborane, but at a slightly higher radius of roughly 30 cm. Thus, subsequent increases in radius beyond this extremum observe significant reductions in k_{eff}. To reach a critical mass, the reactor algorithm will also need to incorporate changes in fuel volume loading or further increase the B-11 enrichment beyond 99.9%. The current loading pattern is taken on a per fuel assembly basis to minimize the radial power peaking while maintaining criticality. A similar methodology can be performed using alternative propellants, but it will require in-depth optimization techniques that are outside the scope of this paper. While this analysis is excluded from this work, it will be a focus for near-term modeling to inform critical questions from NASA and the technical community.

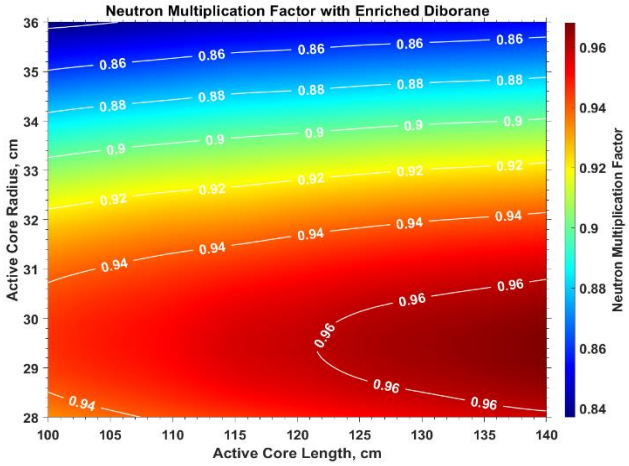

Fig. 6. Geometry Impacts on k_{eff} for Enriched Diborane

IV. CONCLUSIONS

This work analyzed the impact of alternative propellants on the performance of the SNP TRD. This analysis was performed through a coupled engine/reactor algorithm. The propellant options surveyed in this study include ammonia, helium, water, methane, and enriched diborane. Engine performance with alternative propellants were compared to a H_2-engine cycle since this is the reference propellant for current NASA NTP missions. Results in this work include neutron multiplication factor trends given control drum rotation and geometrical changes based on the government TRD.

Key takeaways from this assessment are that methane, helium, and water were found to increase criticality of the reactor, but these options have drawbacks related to channel coking (methane), oxidation (water), and cryogenic storage (helium). Ammonia and enriched diborane, but these options result in a reactivity penalty compared with hydrogen. Parametric studies showed that reactor geometry and fuel volume loading can allow for criticality to be achieved with these reactor designs. All these alternative propellants may be able to decrease overall system mass and increase engine thrust, but the penalty to specific impulse may be too large for some mission architectures. Still, this work has displayed that there are several viable options for NTP without the use of hydrogen. Forward work on this task includes direct coupling between Serpent and the thermal hydraulics in Simulink, assessing different reactor configurations beyond the TRD, and introducing transient engine and reactor performance into the algorithm.

ACKNOWLEDGMENTS

This work was supported by NASA's Space Technology Mission Directorate (STMD) through the Space Nuclear Propulsion (SNP) project. This work was funded under Contract No. 80LARC17C0003. This research made use of Idaho National Laboratory computing resources which are supported by the Office of Nuclear Energy of the U.S. Department of Energy and the Nuclear Science User Facilities under Contract No. DE-AC07-05ID14517.

REFERENCES

[1] S. D. Heister, W. E. Anderson and T. L. Pourpoint, Rocket Propulsion, Cambridge: Cambridge University Press, 2019.

[2] I. H. Bell, J. Wronski, S. Quoilin and V. Pourpoint, "Pure and Pseudo-Pure Fluid Thermophysical Property Evaluation and the Open-Source Property Library CoolProp," *Industrial and Engineering Chemistry Research,* vol. 53, no. 6, pp. 2498-2508, 2014.

[3] E. C. Selcow, R. E. Davis, K. R. Perkins, H. Ludwig and R. J. Cerbone, "Assessment of the Use of H2, CH4, NH3, and CO2 as NTR Propellants," in *American Institute of Physics*, Albuquerque, 1992.

[4] D. Nikitaeva, C. D. Smith and M. Duchek, "Effects of Heat Transfer Coefficient Variation on Nuclear Thermal Propulsion Engine Performance," in *Nuclear and Emerging Technologies for Space*, Idaho Falls, 2023.

[5] D. Nikitaev and D. L. Thomas, "Alternative Propellant Nuclear Thermal Propulsion Engine Architectures," *Journal of Spacecraft and Rockets,* 2022.

[6] D. Nikitaev and D. L. Thomas, "Impacts of In-Situ Alternative Propellant on Nuclear Thermal Propulsion Mars Vehicle Architectures," *Journal of Spacecraft and Rockets,* vol. 59, no. 6, pp. 2038-2052, 2022.

[7] Los Alamos National Laboratory, "Lib80x— Library based on ENDF/B-VIII.0," 2022.

[8] D. Nikitaev, C. Smith and K. Palomares, "Nuclear Thermal Propulsion Turbomachinery Modeling," in *Nuclear and Emerging Technologies for Space Conference*, Cleveland, 2022.

[9] J. Gustafson, M. Krecicki, R. Swanson, B. Zilka and J. K. .. Witter, "Space Nuclear Propulsion Fuel and Moderator Development Plan Conceptual Testing Reference Design," in *Nuclear and Emerging Technologies for Space*, Virtual Event, 2021.

[10] J. Leppanen, M. Pusa, T. Viitanen, V. Valtavirta and T. Kaltiaisenaho, "The Serpent Monte Carlo code: Status, development and applications in 2013," *Annals of Nuclear Energy,* vol. 82, pp. 142-150, 2015.